



Contents lists available at ScienceDirect

# Journal of Rock Mechanics and Geotechnical Engineering

journal homepage: [www.rockgeotech.org](http://www.rockgeotech.org)

## Review

# A review on the performance of conventional and energy-absorbing rockbolts



Charlie C. Li<sup>a,\*</sup>, Gisle Stjern<sup>a,b</sup>, Arne Myrvang<sup>a</sup>

<sup>a</sup> Department of Geology and Mineral Resources Engineering, Norwegian University of Science and Technology (NTNU), Trondheim 7491, Norway

<sup>b</sup> Statoil ASA, Stavanger, Norway

## ARTICLE INFO

### Article history:

Received 24 October 2013

Received in revised form

9 December 2013

Accepted 11 December 2013

Available online 19 March 2014

### Keywords:

Rockbolt

Laboratory bolt test

Energy-absorbing rockbolt

Yield rockbolt

Pull test

Shear test

Dynamic test

Drop test

## ABSTRACT

This is a review paper on the performances of both conventional and energy-absorbing rockbolts manifested in laboratory tests. Characteristic parameters such as ultimate load, displacement and energy absorption are reported, in addition to load–displacement graphs for every type of rockbolt. Conventional rockbolts refer to mechanical rockbolts, fully-grouted rebars and frictional rockbolts. According to the test results, under static pull loading a mechanical rockbolt usually fails at the plate; a fully-grouted rebar bolt fails in the bolt shank at an ultimate load equal to the strength of the steel after a small amount of displacement; and a frictional rockbolt is subjected to large displacement at a low yield load. Under shear loading, all types of bolts fail in the shank. Energy-absorbing rockbolts are developed aiming to combat instability problems in burst-prone and squeezing rock conditions. They absorb deformation energy either through ploughing/slippage at predefined load levels or through stretching of the steel bolt. An energy-absorbing rockbolt can carry a high load and also accommodate significant rock displacement, and thus its energy-absorbing capacity is high. The test results show that the energy absorption of the energy-absorbing bolts is much larger than that of all conventional bolts. The dynamic load capacity is smaller than the static load capacity for the energy-absorbing bolts displacing based on ploughing/slippage while they are approximately the same for the D-Bolt that displaces based on steel stretching.

© 2014 Institute of Rock and Soil Mechanics, Chinese Academy of Sciences. Production and hosting by Elsevier B.V. All rights reserved.

## 1. Introduction

Rockbolts are widely used today in order to secure underground excavation spaces. Conventional rockbolts include mechanical bolts (i.e. expansion shell bolts), fully-grouted rebars and frictional bolts (such as Split set and inflatable bolts, e.g. Swellex and Omega). Conventional rockbolts are used mainly to deal with instability problems under low or relatively low rock stress conditions. A new category of rockbolt has recently been developed with the aim of combating high-stress induced instability problems such as rock-burst and rock squeezing. This category includes cone bolts,

Garford solid bolts, Roofex, D-Bolts and Yield-Lok bolts, which are here collectively called energy-absorbing rockbolts but referred to as yield bolts in some literature. Based on their coupling mechanism, rockbolts can be classified as continuously mechanically coupled (CMC), continuously frictionally coupled (CFC), or discretely mechanically or frictionally coupled (DMFC) (Windsor, 1997). Fully-grouted rebars are mechanically bound to the grout/rock through the tiny ribs on the cylindrical surface of the bolt shank and are thus a type of CMC bolt. Split set and inflatable bolts such as Swellex and Omega are CFC bolts, since they are bound to the rock mass mainly via friction resistance along their entire length. Expansion shell and all energy-absorbing bolts are anchored in boreholes at one or more discrete points and are thus DMFC bolts.

On the other hand, rockbolts can also be classified as stiff, ductile and energy-absorbing from the point of view of bolt performance (Li, 2010). A stiff bolt displaces for a small amount prior to failure. This kind of bolt usually refers to fully encapsulated rebar bolts. It will be seen later in this paper that a fully encapsulated rebar bolt only can displace approximately 30 mm when subjected to fracture opening. The advantage of this type of bolt is its high load capacity which is equal to the strength of the bolt material. A ductile bolt can tolerate a large rock displacement but its load capacity is relatively

\* Corresponding author. Tel.: +47 73594848.

E-mail address: [charlie.c.li@ntnu.no](mailto:charlie.c.li@ntnu.no) (C.C. Li).

Peer review under responsibility of Institute of Rock and Soil Mechanics, Chinese Academy of Sciences.



low. Split set is a typical bolt of this type, which in principle can displace as much as the bolt length at a load level equal to the frictional resistance on the bolt cylindrical surface. An energy-absorbing bolt can carry a load equal or close to the strength of the bolt material and displace for a large amount so that it can absorb a good amount of energy prior to failure.

The performance of a rockbolt is dependent upon the loading conditions to which it is subjected. In situ loading conditions include the opening and shearing of single rock fractures, continuous rock deformation, or various combinations of the two. However, it is impossible, actually not necessary, to simulate every type of loading condition in the laboratory when evaluating the performance of a rockbolt. Among the loading conditions, the pull and shear caused by the movement of a single rock fracture are the most representative loading conditions for rockbolts. Therefore, it is widely acknowledged in the field of rock mechanics that laboratory pull and shear tests are generally the two most appropriate measures with which to examine rockbolt performance. Indeed, a good understanding of rockbolts performance is essential for their appropriate practical application. A great number of static pull and shear tests have been conducted in the Rock Mechanics Laboratory at the Norwegian University of Science and Technology (NTNU), Norway, over the past two decades (e.g. [Stjern, 1995](#); [Dahle and Larsen, 2006](#)). In addition, many dynamic drop tests have also been conducted on energy-absorbing rockbolts, for example, at Canada Center for Mineral and Energy Technology (CANMET), Ottawa, Canada, and Western Australia School for Mines (WASM), Australia, during the past decade, with the first author involved in a number of these tests. The results of the tests, as well as some by others, are presented in this paper with the aim of providing a systematic illustration of the performances of all types of rockbolts.

## 2. Rockbolt loading models

The loading condition of a rockbolt is associated with its anchoring mechanism. Analytical loading models for conventional rockbolts were established by [Li and Stillborg \(1999\)](#) and [Li \(2008\)](#). In addition to these models, loading models for energy-absorbing rockbolts are proposed in this section. Such models are helpful in interpreting variation in test results between different types of rockbolts.

### 2.1. Two-point anchored rockbolts

An expansion shell bolt is a typical two-point anchored support device composed of a solid shank and an expansion shell at the far end of the bolt ([Fig. 1](#)). Anchoring of the bolt is achieved through friction and interlocking between the expansion shell and the borehole wall. The load-bearing capacity of this type of bolt is dependent upon both the tightness of the expansion shell and the strength of the rock. Vibrations and stress relaxation may lead to partial or entire loss of anchoring. Another type of two-point anchored bolt involves the far end of the bolt being grouted with resin, which guarantees more reliable anchoring than the expansion shell bolt.

Under a pull load at the bolt head, the shank of the bolt is stretched identically in every cross-section, resulting in a constant axial stress along the length of the bolt, as shown in [Fig. 1](#). The shear stress on the shank surface is obviously zero because of the hollow annulus in the hole.

### 2.2. Fully-grouted rebar bolts

Fully-grouted rebar bolts are bound to the grout/rock via ribs on the bolt surface, with the main anchoring mechanism of the mechanical interlocking between the ribs and hardened grout. This

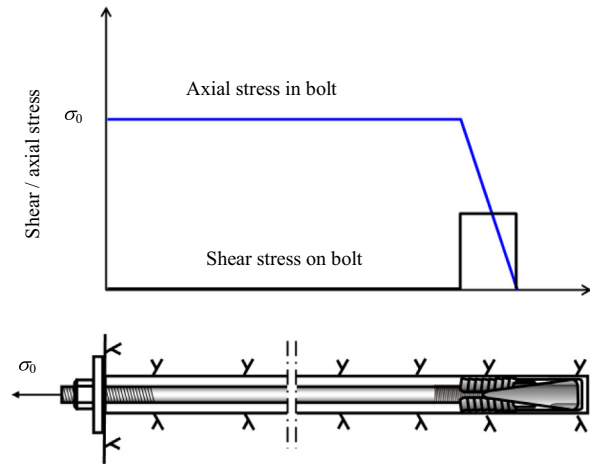


**Fig. 1.** Stress distributions along the length of a two-point anchored bolt when subjected to a pull load at the bolt head.

type of bolt is characterised by its reliable anchoring and high load capacity.

When the bolt is subjected to a pull load at the bolt head, the load is simply transferred to the rock by the ribs. The axial load in the bolt decreases with distance from the loading point when the applied load is low. Bond failure will commence at the loading point when the applied load is beyond a certain level, propagating toward the far end of the bolt with an increase in the applied load. The residual shear stress on the bolt surface depends on the extent of the failure at the bolt–rock interface. The general pattern of shear stress on the bolt surface is illustrated in the theoretical model shown in [Fig. 2](#). In the model, the bond fails completely in the section immediately adjacent to the loading point, resulting in zero residual shear stress on the bolt surface. No bond failure occurs at the bolt–rock interface beyond the peak shear stress. The bond at the interface deforms elastically, with shear stress attenuating to zero with increasing distance from the loading point. The maximum axial load always occurs at the loading point. Laboratory tests have shown that the length of the de-bonding section is approximately 150 mm for a rebar with cement grout when the axial load reaches the strength of the bolt material. The advantage of rebar bolts is their high load capacity while the disadvantage is the high stiffness.

### 2.3. Frictional rockbolts

Split set and inflatable bolts (e.g. Swellex and Omega) belong to the class of frictional bolt ([Fig. 3](#)). A frictional bolt interacts with the

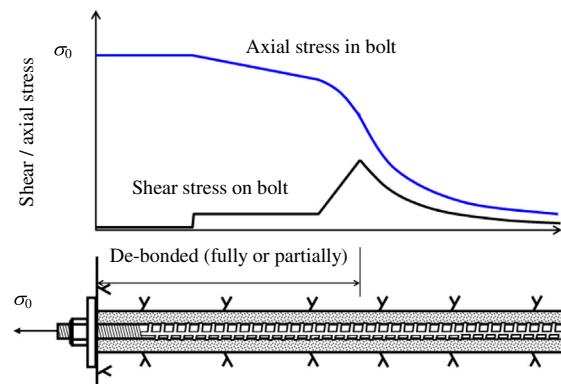


**Fig. 2.** Stress distributions along the length of a fully-grouted bolt when subjected to a pull load at the bolt head.



Fig. 3. Split set and inflatable rockbolts.

rock via friction at the bolt–rock interface along its entire length. When it is subjected to a pull load at the bolt head (Fig. 4), the shear strength at the interface will be first mobilised at the loading point. The bolt starts to slip outward in the strength-mobilised section, with the length of the slipping section increasing with the increase of the applied load. The shear stress on the slipping section of the bolt remains approximately to the level of the shear strength during bolt displacement. Because of this characteristic, frictional bolts can accommodate large rock deformation without significant loss of their load-bearing capacity.

In theory, the ductile performance of this type of bolt is able to be achieved only when frictional slippage occurs along the entire length of the bolt. In reality, the slippage is only guaranteed for Split set because of its special installation procedure. In installation, Split set is pushed, for instance by a bolting rig, into the borehole. The push load has to be limited to a relatively low level in order to avoid buckling of the Split set tube. In theory, the pull load capacity of a Split set is equal to the maximum push load in installation. Both field and laboratory tests show that the load capacity of a Split set is approximately 50 kN/m (Cheng and Feng, 1983; Myrvang and Hanssen, 1983; Player et al., 2009). Therefore, it is said that the

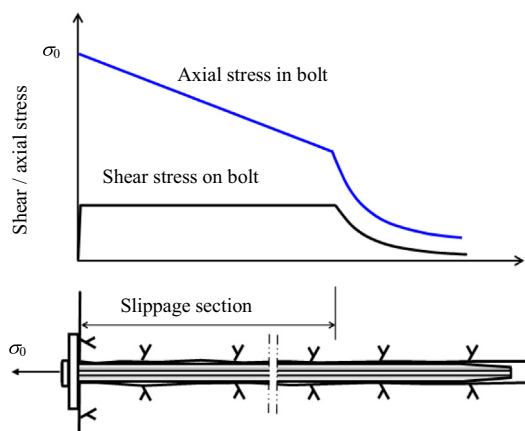


Fig. 4. Stress distributions along the length of a frictional bolt when subjected to a pull load at the bolt head.

Split set can accommodate large rock deformations but has a low load capacity.

An inflatable bolt is installed by expanding the folded tube to match the size of the borehole. Its load capacity is not only associated with the contact stress between the bolt tube and the borehole wall (resulting in frictional resistance) but also with the roughness of the borehole wall (resulting in mechanical interlocking). An inflatable bolt is maximum loaded in the bolt head if subjected to a load applied at the bolt plate as illustrated in Fig. 4. The bolt tube will slip if the bolt length is short enough and the load capacity is equal to the unit frictional-and-interlocking force times the bolt length. Slippage will not occur and the tensile strength of the bolt tube will be mobilised if the bolt length is long enough. In this case, the pull load capacity of the bolt is high but its displacement capacity would be simply limited to the stretch of the tube.

#### 2.4. Energy-absorbing rockbolts

Energy-absorbing rockbolts are loaded in different ways when subjected to loading, depending on their anchoring mechanisms. The loading model for two-point anchored energy-absorbing rockbolts, such as the cone bolt, Garford bolt, Roofex and Yield-Lok, is similar to that of conventional two-point anchored rockbolts (Fig. 5a), with the main difference being that the energy-absorbing rockbolts yield at predefined load levels. The loading of multi-point anchored D-Bolts is different from that of other energy-absorbing rockbolts, in that the opening of a rock fracture only induces load in the section of the D-Bolt that overrides the fracture (Fig. 5b). The yield and ultimate loads of the bolt are equal to the corresponding strengths of the bolt steel. The bolt absorbs deformation energy by fully mobilising the deformation capacity of the steel along the entire length of the bolt section.

### 3. Testing methods

#### 3.1. Static pull test

Ultimate load and maximum displacement are two important parameters with which to describe bolt performance. In the laboratory, the load and displacement capacities of a bolt are evaluated through static pull and shear tests, and the principles of which are illustrated in Fig. 6. When tested, the rockbolt is installed in the hole of two blocks (or tubes). After the load is applied to the blocks, the load and the joint opening of the two blocks are registered.

Fig. 7a shows an oblique sketch of the bolt test rig that was employed for the pull and shear tests carried out in the Rock Mechanics Laboratory at NTNU. Two pieces of high strength concrete blocks, both with dimensions of 950 mm × 950 mm × 950 mm, are placed in the frame of the test rig. A hole is drilled through the blocks in place, with the bolt then installed in the borehole. For a pull test, the pull load is applied to the right concrete block (in Fig. 7b) through two hydraulic jacks, while the left block is fixed in the frame. For a shear test, the right block is fixed and the left block is pushed laterally with a hydraulic jack located at the joint of the two blocks. The load capacity of the bolt test rig for pull and shear tests is 600 kN and 500 kN, respectively.

#### 3.2. Dynamic drop test

The dynamic performance of a rockbolt is often described in terms of impact velocity and kinetic energy input. The split tube test is usually carried out to measure the energy absorption of a rockbolt, as shown in Fig. 8, with the bolt encapsulated in the tubes

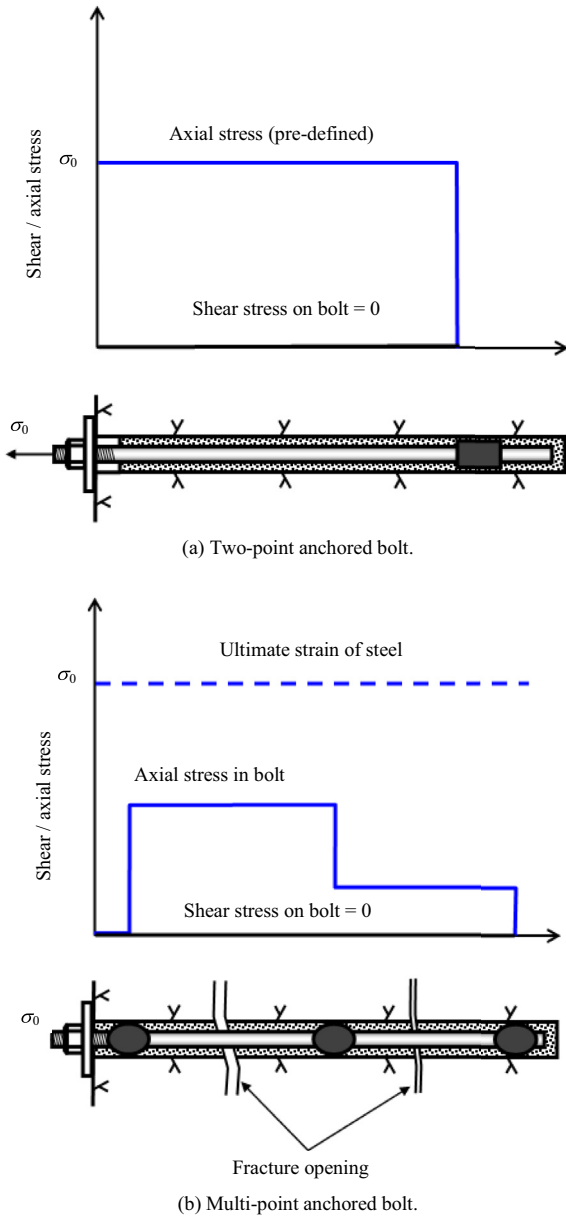


Fig. 5. Stress/strain distributions along energy-absorbing bolts when subjected to pull loading.

with grout. Two methods are available with which to apply the dynamic load to the tested bolt. The first is the free-fall method, in which the upper tube is fixed on the ceiling and a mass freely falls onto the impact plate attached to the lower tube (Fig. 8a). Kinetic energy is transferred to the bolt via the plate and the lower tube. The test facility at CANMET in Ottawa, Canada, employs this method to apply the dynamic load. The second method involves momentum transfer. In this method, the mass and split tubes fall freely together until the stopper at the upper end of the split tubes meets a stationary beam (Fig. 8b). The movement of the assembly is then stopped, with the momentum and kinetic energy then transferred to the bolt via the plate and the lower tube.

4. Static testing of conventional rockbolts

A large number of pull and shear tests have been carried out on rockbolts using the bolt test rig shown in Fig. 7 since the middle of

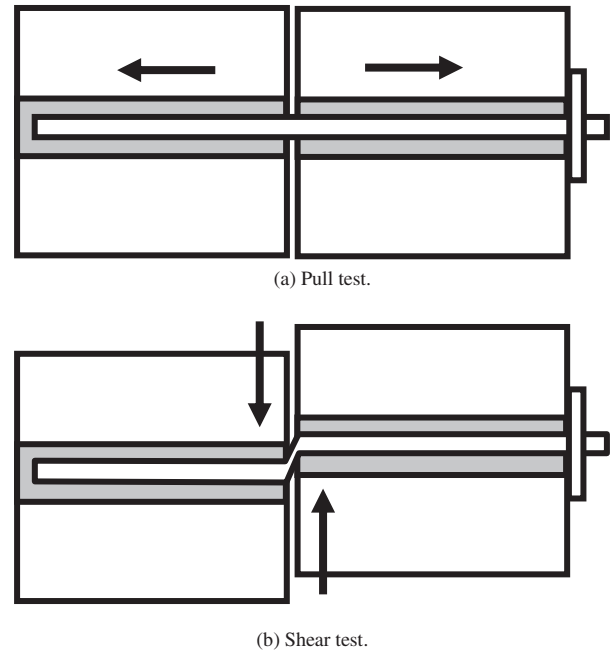


Fig. 6. Sketches illustrating the principles of rockbolt static pull and shear tests.

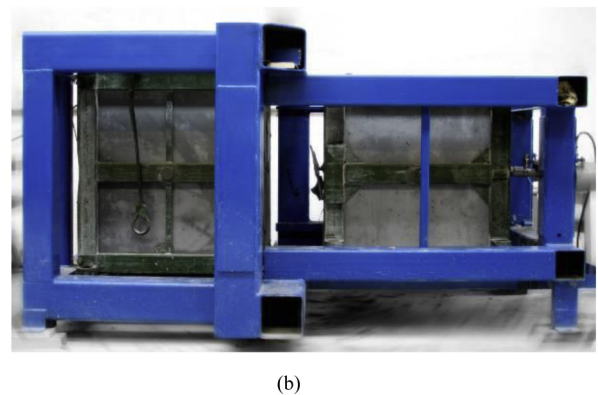
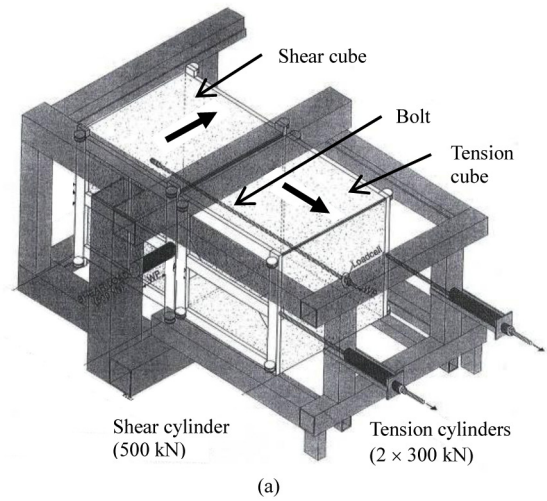


Fig. 7. The test rig for static pull and shear tests in the Rock Mechanics Laboratory at NTNU. The sizes of both concrete blocks are 950 mm × 950 mm × 950 mm. (a) An oblique sketch of the test rig (Stjern, 1995); and (b) The front view of the test rig.

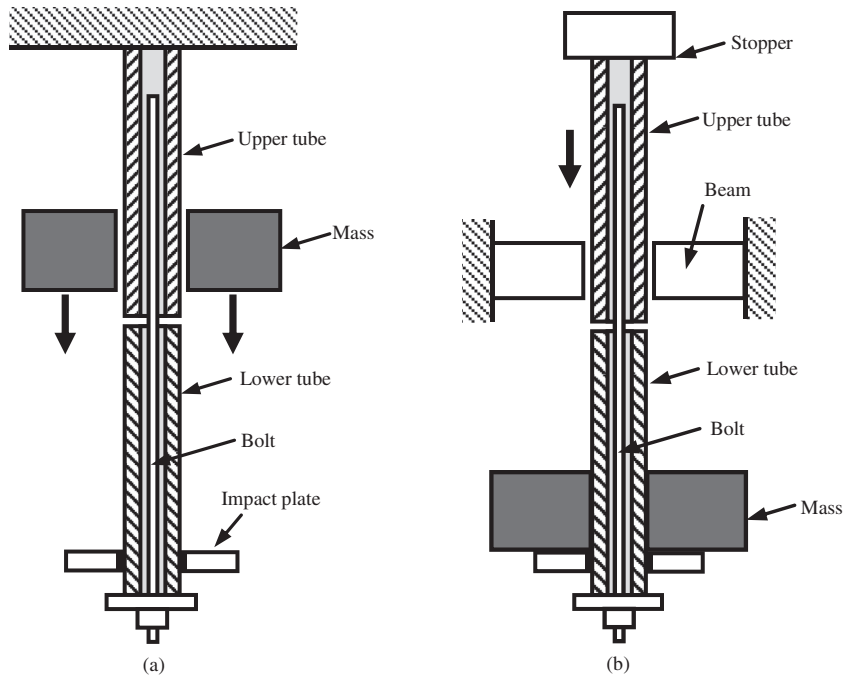


Fig. 8. Two principles of rockbolt dynamic drop tests. (a) Mass free-fall; and (b) Momentum transfer.

the 1990s, for example by [Stjern \(1995\)](#) and by [Dahle and Larsen \(2006\)](#). Test results for the studied rockbolt types are presented in this section.

4.1. Mechanical bolts

A rebar 20 mm in diameter was point-anchored in a hole drilled in the concrete blocks, with an expansion shell positioned at the far end of the bolt. Deformation occurred in both the plate and the bolt shank during the pull test. Under pull loading, the bolt finally failed in the thread at an ultimate load of 160 kN and total displacement of 55 mm ([Fig. 9a](#)). Shank elongation accounted for only approximately 14 mm of total displacement, with the rest attributed to the elongation of the thread and the deformation of the plate. Under shear loading, the bolt finally failed in the shank at the joint. The ultimate shear load was 217 kN and the total shear displacement was 110 mm ([Fig. 9b](#)).

4.2. Fully-grouted rebar bolts

A rebar 20 mm in diameter was fully grouted with cement mortar in a borehole of 32 mm in diameter. The water–cement ratio of the mortar was 0.32. Under pull loading, the bolt finally failed in the bolt shank at the joint ([Fig. 10a](#)). The ultimate pull load was 205 kN and the maximum pull displacement was 40 mm. Under shear loading, the bolt also failed in the shank at the joint ([Fig. 10b](#)). The ultimate shear load was 199 kN and the total shear displacement was 47 mm.

4.3. Frictional rockbolts

A piece of Split set SS46, 46 mm in diameter, was pushed into a borehole of diameter 42.3 mm. Under pull loading, the bolt did not fail in the bolt shank but rather slipped in the hole ([Fig. 11a](#)). The pull load reached its ultimate value of 51 kN after only a few

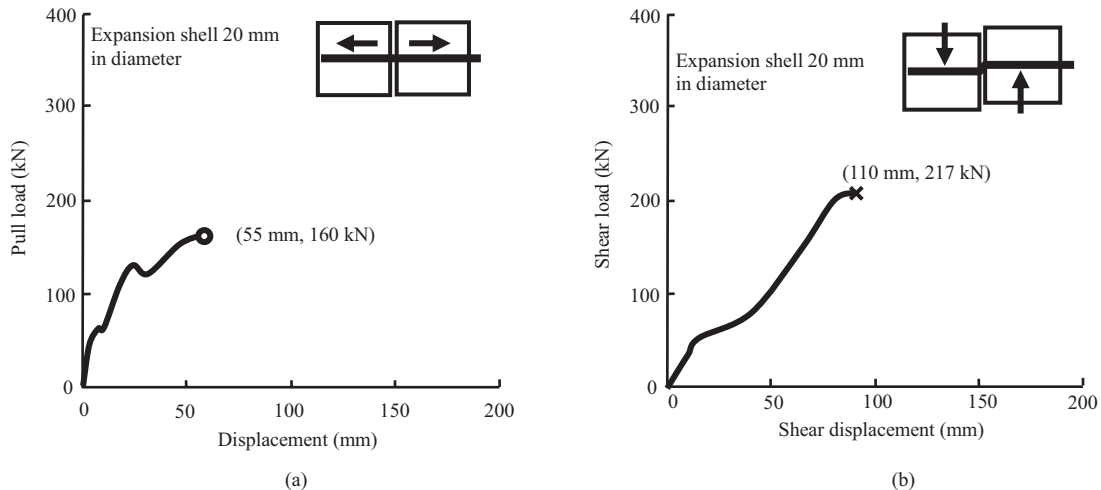


Fig. 9. Load–displacement behaviour of a mechanical bolt under pull and shear loads. The symbols “o” and “x” refer to failure in the plate and bolt shank, respectively ([Stjern, 1995](#)).

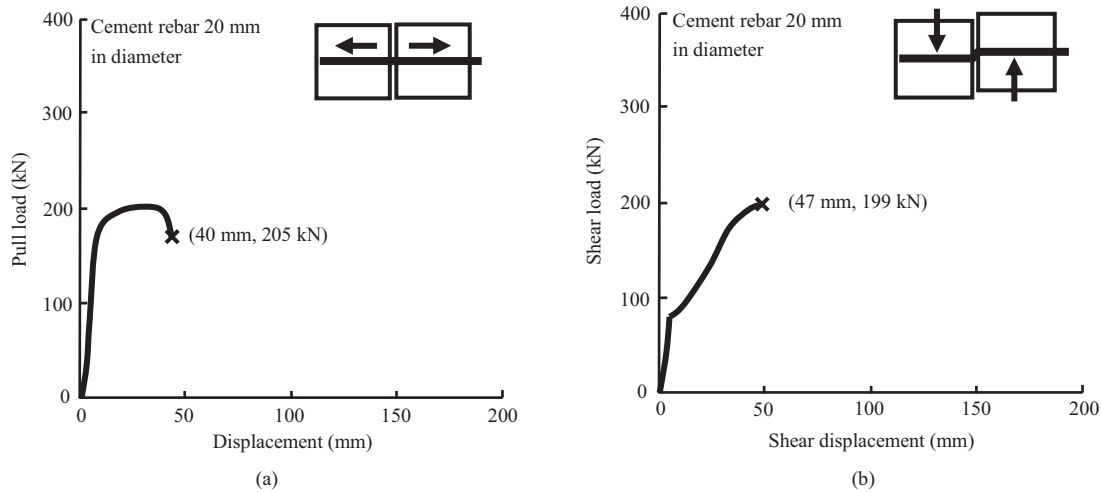


Fig. 10. Load–displacement behaviour of a cement fully-grouted rebar under pull and shear loads. Symbols as Fig. 9 (Stjern, 1995).

millimetres of displacement. Under shear loading, the bolt failed in the shank at the joint of the concrete blocks (Fig. 11b), with shank failure occurring at an ultimate shear load of 160 kN and a shear displacement of 68 mm.

A piece of inflatable bolt, 38 mm in diameter before unfolding, was installed in a borehole of diameter 48 mm. Under pull loading, the bolt did not fail in the bolt shank but rather slipped in the hole (Fig. 12a). The pull load reached its ultimate value 121 kN after a pull displacement of 26 mm and then gradually decreased with the increase of the pull displacement. Under shear loading, the bolt failed in the bolt shank at the joint (Fig. 12b). The ultimate shear load was 179 kN and the final total shear displacement 59 mm.

4.4. Twin strand cable

A twin strand cable, 2 × 12.7 mm in diameter, was cement grouted in a borehole. The ultimate tensile strength of the twin cable was approximately 380 kN. Under pull loading, the cable started to slip, i.e. yielded at 170 kN after a small displacement of approximately 25 mm (Fig. 13a). Load increased gradually with displacement, possibly because of the dilation effect at the grout–strand interface, eventually reaching 210 kN after a displacement of 250 mm. The cable didn't fail when the test was terminated at that

point. Under shear load, the wires in the twin strand cable failed in tensile mode. The ultimate shear load was 233 kN, approximately 60% of the tensile strength, with a shear displacement of 134 mm (Fig. 13b).

4.5. Fibre glass bolt

A fibre glass bolt 22 mm in diameter was fully grouted with cement mortar in a 45 mm diameter borehole. Under pull loading, the bolt failed in the bolt shank at the joint. The ultimate pull load was 380 kN and the maximum pull displacement was 37 mm (Fig. 14a). Under shear load, the bolt failed too in the shank at the joint, with the ultimate shear load of 140 kN and the total shear displacement of 33 mm (Fig. 14b).

5. Static and dynamic tests of energy-absorbing rockbolts

5.1. Cone bolt

Invented in South Africa (Jager, 1992; Ortlepp, 1992), the cone bolt was the first yield support device developed to combat rock-burst problems in deep mines. The original cone bolt was designed for cement grout. It consists of a smooth steel bar with a flattened conical flaring forged on to the far end (Fig. 15a). The cone bolt was

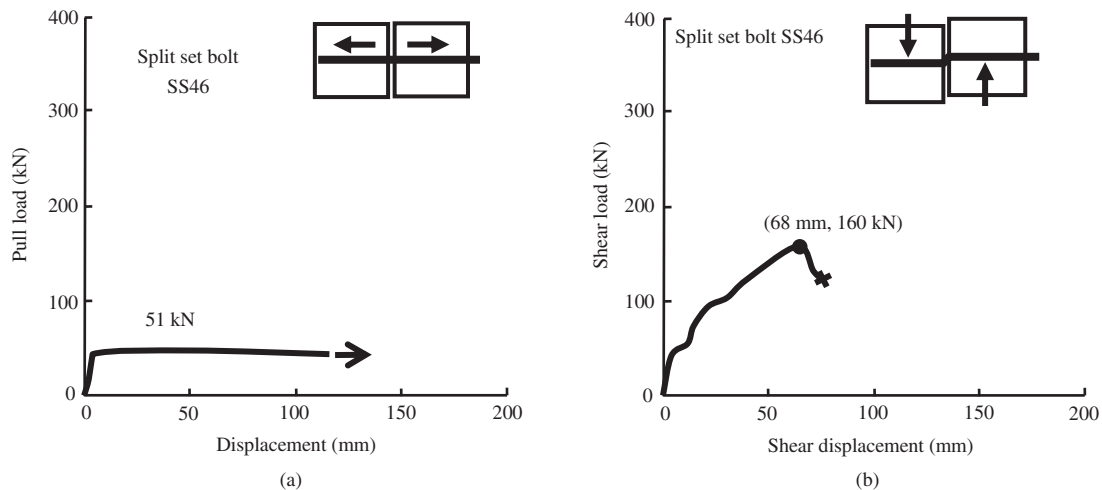


Fig. 11. Load–displacement behaviour of a Split set under pull and shear loads. Symbols as Fig. 9 (Stjern, 1995).

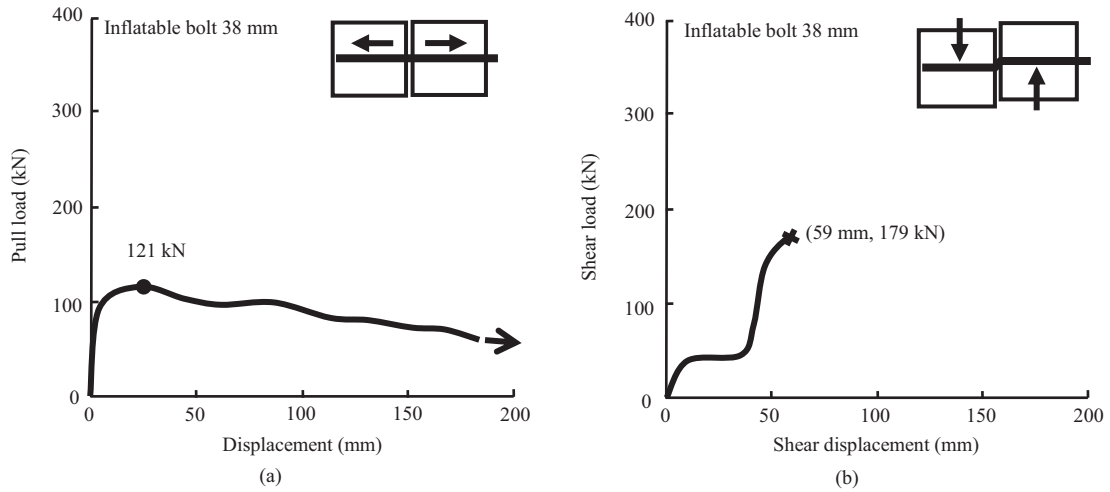


Fig. 12. Load–displacement behaviour of a 38-mm inflatable bolt under pull and shear loads. Symbols as Fig. 9 (Stjern, 1995).

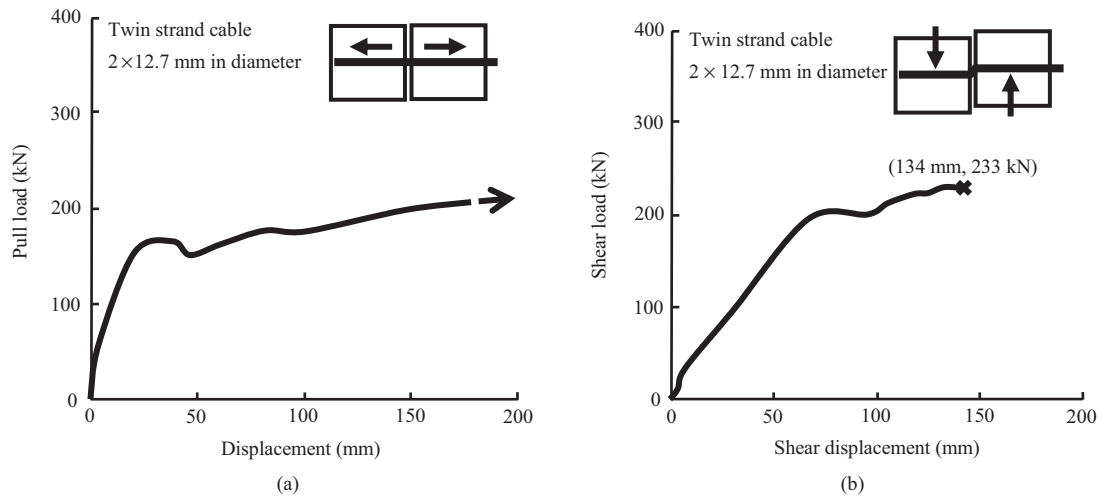


Fig. 13. Load–displacement behaviour of a twin strand cable under pull and shear loads. Symbols as Fig. 9 (Stjern, 1995).

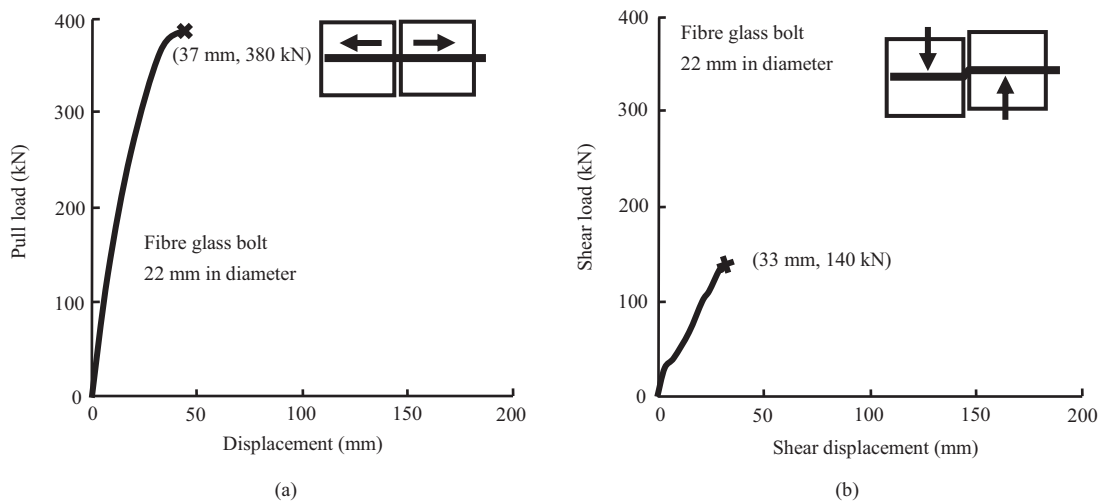


Fig. 14. Load–displacement behaviour of a fibre glass bolt under pull and shear loads. Symbols as Fig. 9.

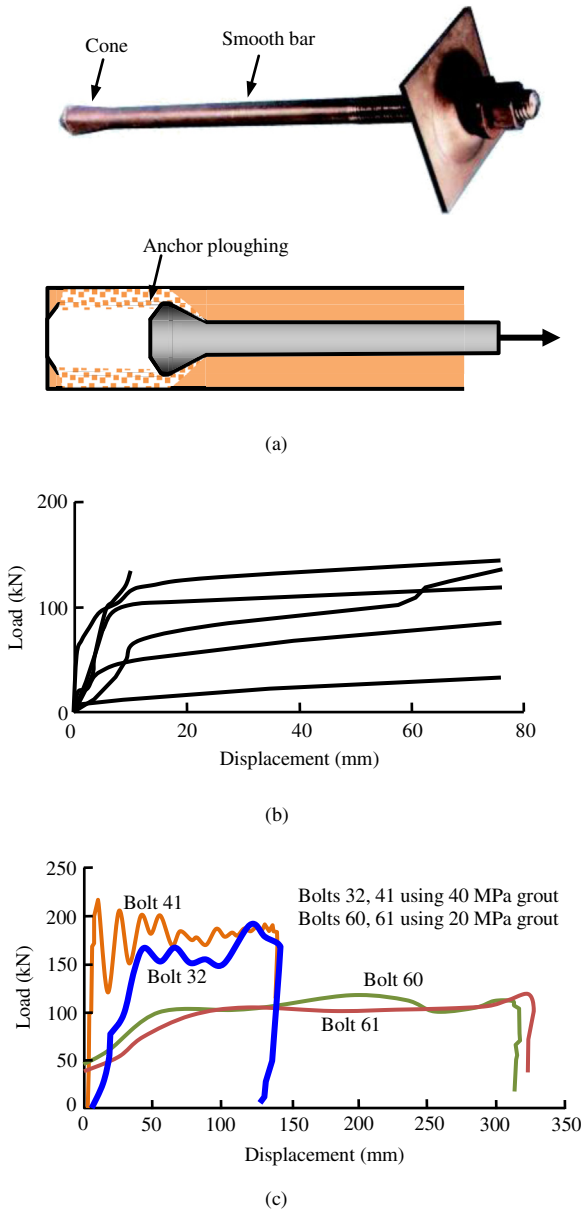


Fig. 15. Static and dynamic test results of resin-grouted cone bolts. (a) The bolt and work principle; (b) Static pull test results of rockbolts, redrawn after Simser et al. (2006); (c) Dynamic drop test results, redrawn after Varden et al. (2008).

modified later for resin grout in Canada (Simser, 2001). The modified cone bolt (MCB) is different from the cement version in that a blade is added at the end of the cone for the purpose of resin mixing. The bolt is designed so that rock dilation between the cone and the face plate of the bolt induces a load on the latter, which then pulls the conical end of the bolt through the grout to do work and absorb energy released from the rock. A cone bolt can displace for a considerable amount if it works in ploughing as intended. Lindfors (2000) carried out a series of pull tests on cement-grouted cone bolts in an underground mine in Sweden. The bolts displaced up to 900 mm at a load level of approximately 170 kN. However, whether the ploughing occurs or not is dependent upon not only the shape and size of the cone, but also the strength of the hardened grout. The static and dynamic tests on modified cone bolts showed that the load capacity of the cone bolt varies in a wide range (Fig. 15b and c). Fig. 15c shows the dynamic test results of 22-

mm cone bolts which were impacted with a kinetic energy input of 33 kJ. The ultimate dynamic load of the bolts was 150–175 kN for the 40 MPa grout, but dropped to approximately 100 kN for the 20 MPa grout.

5.2. Garford solid bolt

Invented in Australia, the Garford solid bolt consists of a solid steel bar, an anchor and a coarse-threaded steel sleeve at the far end (Fig. 16a). This bolt is characterised by its engineered anchor, the inner diameter of which is smaller than the diameter of the solid bolt bar. The anchor is resin encapsulated in a borehole. When the rock dilates, the solid bar is extruded through the hole in the anchor at a predefined pull load. Fig. 16b shows the dynamic test results of two 20-mm bolts loaded with a kinetic energy input of 33 kJ (Varden et al., 2008).

5.3. Roofex bolt

Roofex bolts are also composed of an engineered anchor and a smooth bar (Fig. 17a) (Charette and Plouffe, 2007; Galler et al., 2011), with the work principle similar to that of the Garford solid bolt. The anchor is again resin encapsulated in a borehole, with the smooth bar slipping through the anchor to accommodate rock displacement. Laboratory test results for Roofex bolts are shown in Fig. 17b and c.

5.4. D-Bolt

Invented in Norway, the D-Bolt comprises a smooth steel bar and a number of integrated anchors along the bolt length (Fig. 18a)

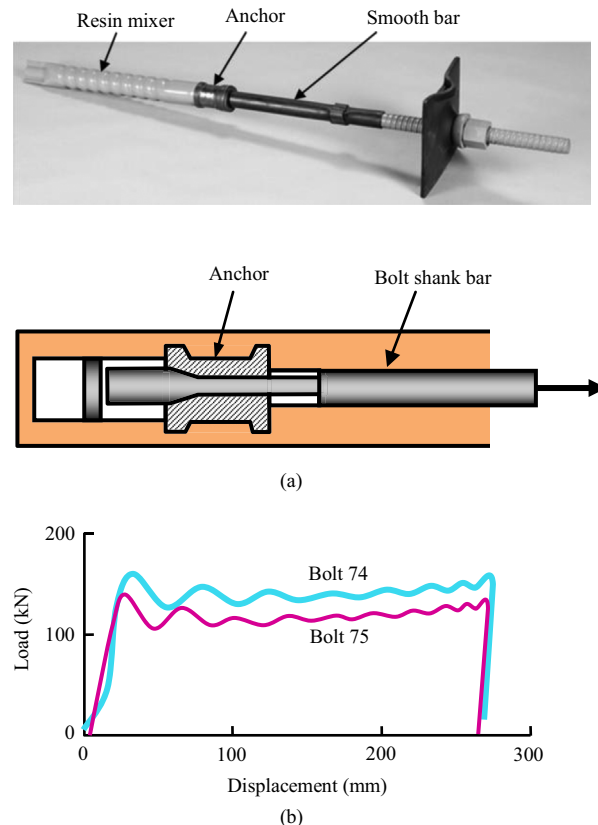
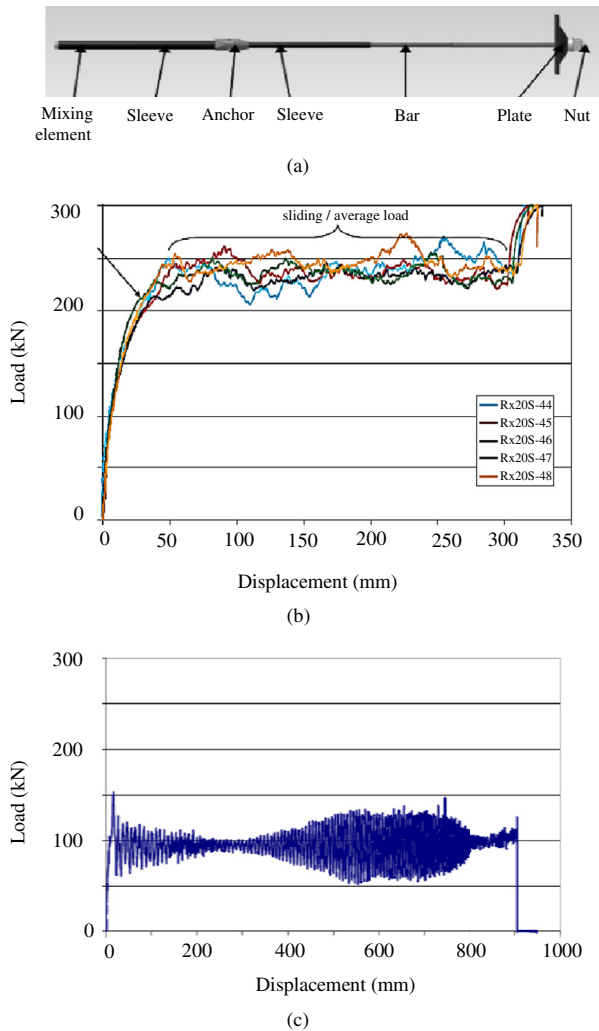


Fig. 16. (a) Garford solid bolt and work principle; (b) Dynamic test results of 20-mm bolts with impact input of 33 kJ. Curves redrawn after Varden et al. (2008).





**Fig. 17.** Roofex Rx20 bolt and test results (Galler et al., 2011). (a) The bolt and work principle; (b) Static pull test results of rockbolts; (c) Dynamic test result.

(Li, 2010). The bolt is either cement or resin encapsulated in a borehole. The anchors are firmly fixed in the grout, while the smooth bar sections between the anchors elongate upon rock dilation. The bolt absorbs energy by fully mobilising the strength and deformation capacity of the bolt steel. Static and dynamic performance data for the D-Bolt are shown in Fig. 18b and c. Bolt ultimate load is equal to the tensile strength of the steel, while bolt ultimate displacement is approximately 15% of bolt length. Taking a bolt section of  $\phi 22 \text{ mm} \times 1500 \text{ mm}$  as an example, the ultimate static load and displacement are 260 kN and 165 mm, respectively, and the ultimate dynamic load and displacement are 285 kN and 220 mm, respectively. The bolt section absorbs approximately 60 kJ of energy prior to failure under dynamic loading. Every section of the bolt works independently; the failure of one section does not result in the loss of the entire bolt, with the remaining sections continuing to provide rock reinforcement.

### 5.5. Yield-Lok bolt

The Yield-Lok bolt consists of a 17.2 mm round steel bar (Fig. 19a). The anchor, or Upset, of the bolt is encapsulated in an engineered polymer coating. The bolt is grouted in the borehole,

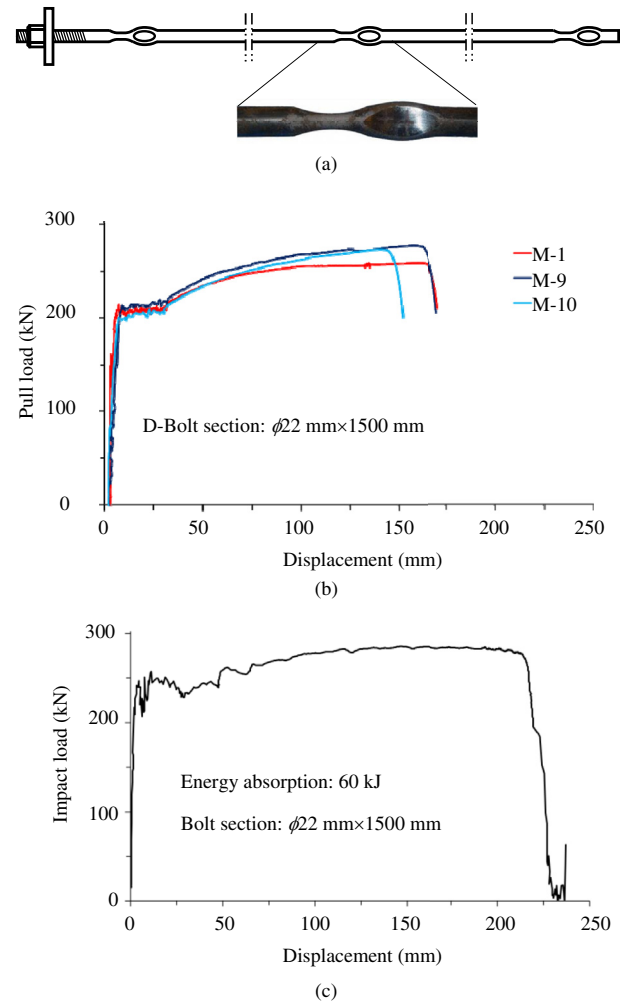


**Fig. 18.** D-Bolt and test results of a bolt section of 22 mm  $\times$  1.5 m (Li, 2012; Li and Doucet, 2012). (a) The bolt, (b) static pull test results of rockbolts, and (c) dynamic test result.

with the Upset ploughing in the polymer coating when the bolt load exceeds the predefined load level. Static and dynamic performance data for the bolt are shown in Fig. 19b and c. The dynamic load is in general lower than the static load.

## 6. Discussion

### 6.1. On the conventional rockbolts

The load capacity of a mechanical rockbolt is mainly dependent upon the strength of the face plate and bolt thread, as well as the tightness of the expansion shell. As a result, the load and deformation capacities of this type of rockbolt may vary in a large range. Two-point anchored bolts often lose their support function due to failure of the face plate or thread when subjected to pull loading (Fig. 9a). Under shear loading, the bolt shank can be locked by the friction between the shank and the rock, with failure occurring in the bolt steel (Fig. 9b).

The load capacity of fully-grouted rebar bolts is the highest of the conventional rockbolts, with failure taking place in the bolt shank under both pull and shear loading. This type of bolt is characterised by high load capacity and small displacement (Fig. 10). In other words, fully-grouted rockbolts are strong but stiff.

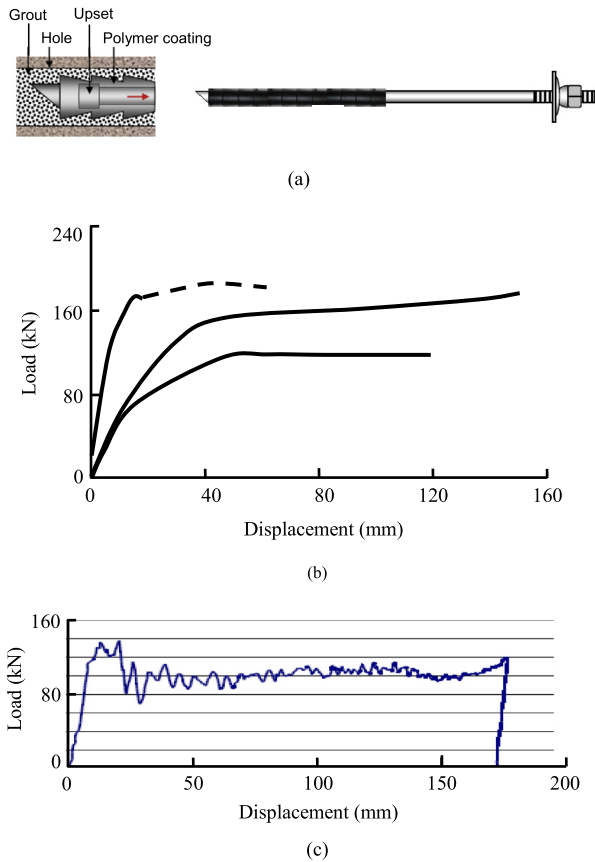


Fig. 19. Yield-Lok bolt and test results, redrawn after Wu et al. (2010). (a) The bolt, (b) static pull test results of rockbolts, and (c) dynamic test result.

Frictional bolts are anchored in the rock mass through the friction between bolt and rock, with frictional resistance dependent upon the contact stress and the contact condition at the bolt–rock interface. The pull load capacity of Split set is low because of the low contact stress at the interface (Fig. 11a). The shear load capacity of Split set is higher than its pull load capacity because of the mechanical locking of the tube (Fig. 11b). In addition to frictional resistance, mechanical interlocking at the bolt–rock interface also contributes significantly to the pull load capacity of this type of bolt. The pull load capacity of an inflatable bolt is larger than that of Split set because of the superposition of the friction resistance and the mechanical locking at the bolt–rock interface (Fig. 12a). Similar to Split set, inflatable bolt fails in the tube steel under shear loading and its shear load capacity is larger than the pull load capacity.

Although the pull load capacity of a fibre glass bolt is approximately two times the strength of a rebar bolt, its shear load capacity is low (Fig. 14). Furthermore, fibre glass bolts are stiff and they accommodate only a very small displacement prior to failure.

## 6.2. On the critical embedment length for frictional and cable bolts

Although both frictional bolts and twin strand cables slide under pull loading (Figs. 12 and 13), this slippage is not an intrinsic characteristic as its occurrence depends on embedment length. Every bolt/cable of this type has a critical embedment length, with slippage taking place only when the embedment length of the bolt

is shorter than this critical length. The critical embedment length ( $L_c$ ) is determined by the tensile strength ( $T$ ) of the bolt/cable shank and the frictional strength ( $R$ ) of the bolt–rock interface:

$$L_c = T/R \quad (1)$$

where  $L_c$  is measured in metres,  $T$  in kN and  $R$  in kN/m. As the embedment length of the bolts/cables tested was 0.95 m, back-calculation produces a frictional strength value of  $R = 121 \text{ kN}/0.95 \text{ m} = 127 \text{ kN/m}$  for the inflatable bolt (Fig. 12a). The tensile strength of an inflatable bolt 38 mm in diameter is typically 190 kN, with the critical embedment length obtained from the above equation thus  $(190/127) = 1.5 \text{ m}$ . The tensile strength of the twin-strand cable tested is 380 kN. According to Fig. 13a, its frictional strength is  $R = 170 \text{ kN}/0.95 \text{ m} = 179 \text{ kN/m}$  and the critical embedment length thus  $(380/179) = 2.1 \text{ m}$ . Both the inflatable bolt and the twin strand cable slipped because their embedment lengths (both 0.95 m) were shorter than their critical embedment lengths (1.5 m for the inflatable bolt and 2.1 m for the cable). Slippage would not occur if their embedment lengths were longer than their critical lengths.

## 6.3. Energy-absorbing rockbolts

All the studied energy-absorbing rockbolts with the exception of the D-Bolt deform based on mechanisms involving bolt shank slippage either in the grout (the cone bolt and the Yield-Lok) or through the anchor (Garford and Roofex bolts). A common characteristic of the slippage-based bolts is that their ultimate dynamic loads are smaller than their static loads (Figs. 17 and 19). In contrast, the D-Bolt absorbs energy through fully mobilising the strength and deformation capacities of the bolt steel. The static and dynamic load capacities of the D-Bolt are fairly similar (Fig. 18).

The performance of an energy-absorbing bolt is characterised by its energy absorption and displacement capacity. When absorbing the same amount of energy, the bolt exhibiting the least displacement is preferred since it is more efficient in restraining rock movement. Table 1 lists the energy absorption, displacement capacity and average dynamic load capacity of selected energy-absorbing rockbolts. Note that the average dynamic load of the listed bolt devices is calculated from the energy absorption and ultimate displacement of the bolts, with the exception of those marked by stars. Energy absorption refers to the total energy absorbed by the bolt prior to failure. For the dynamic test facilities described in Section 3.2, energy absorption is calculated as the sum of the kinetic energy input and an extra amount of energy associated with the displacement of the bolt. The average load is calculated by either of the expressions below:

$$P_{ave} = \frac{E_{tot}}{d} \text{ or } P_{ave} = \frac{E_k}{d} + mg \quad (2)$$

where  $P_{ave}$  represents the average dynamic load,  $E_{tot}$  the total energy absorbed (i.e. the energy absorption),  $E_k$  the kinetic energy input,  $d$  the displacement of the bolt,  $m$  the weight of the drop mass and  $g$  the gravity acceleration.

It can be seen from Table 1 that the average dynamic load of cone bolts varies in a large range from 50 kN to 216 kN. This large spread in values is possibly due to the different displacement mechanisms involved (ploughing, steel stretch or a combination of the two). The average load varies between 120 kN and 156 kN for the Garford solid bolt and between 81 kN and 99 kN for the Yield-Lok. In contrast, the average load of the D-Bolt is considerably more consistent at around 280 kN.

**Table 1**  
Energy absorption, ultimate displacement and average load of energy-absorbing rockbolts under dynamic loading.

Bolt type	Diameter (mm)	Kinetic energy (kJ)	Absorbed energy (kJ)	Drop mass (kg)	Ultimate displacement (mm)	Average load (kN)	References
Cone bolt	22		33.0		190	174 <sup>a</sup>	Varden et al. (2008)
			33.0		190	150 <sup>a</sup>	
			33.0		320	100 <sup>a</sup>	
Cone bolt MCB33 new	17.2	26.3		1184	640	53	Cai and Champaigne (2010)
				1184	520	62	
				2229	465	92	
				1115	420	50	
				1115	335	60	
Cone bolt MCB33 old	17.2	16.4		1115	280	70	
				1115	245	78	
				1115	170	107	
				1115	80	216	
				1115	80	216	
Garford solid bolt			33.0		270	140 <sup>a</sup>	Varden et al. (2008)
			33.0		270	120 <sup>a</sup>	
			21.0		170	124	
			28.0		180	156	
			27.0		195	138	
Roofex Rx20		16.0		893	182	98	Galler et al. (2011)
				1783	412	100	
				2229	592	95	
				2897	703	94	
				2897	785	103	
D-Bolt (0.9-m section)	22	26.0		2452	140	281	Li and Doucet (2012)
				2897	840	108	
				2897	840	108	
D-Bolt (1.5-m section)	22	56.0		2897	225	277	Wu et al. (2010)
Yield-Lok	17.2	16.4		1115	175–230	99–81	

Note: <sup>a</sup> Readings on load–displacement curves.

Frictional bolts, i.e. Split sets and inflatable bolts, are still employed to deal with stress-induced instability problems in a number of underground projects at present. Their energy absorption, displacement and dynamic load capacity are listed in Table 2. The average dynamic load of Split sets and inflatable bolts varies at 5–55 kN and 31–128 kN, respectively. In general, the dynamic load of a frictional bolt is smaller than its static load. According to the test results by Player et al. (2009), the average dynamic load of a friction rock stabiliser is approximately 50% of its static load.

#### 6.4. Conventional rockbolts versus energy-absorbing rockbolts

The performances of conventional and energy-absorbing rockbolts are summarised in Fig. 20. Conventional rockbolts are

characterised by their load capacity (i.e. rebar) or ductility (i.e. frictional bolts). The area under the load–displacement curve of a rockbolt represents the energy absorption of the bolt. All conventional rockbolts have low energy-absorbing capacities. According to Kaiser et al. (1996), the dynamic energy absorption of a 19-mm resin-grouted rebar bolt and a 16-mm mechanical bolt is only 1–4 kJ and 2–4 kJ, respectively. In contrast, energy-absorbing rockbolts are characterised by their high load and displacement capacities, with energy absorption usually significantly larger than that of conventional rockbolts.

**Table 2**  
Energy absorption, ultimate displacement and average load of frictional rockbolts under dynamic loading (Player et al., 2009; Hadjigeorgiou and Potvin, 2011).

Bolt type	Absorbed energy (kJ)	Ultimate displacement (mm)	Average yield load (kN)
Split set SS46 (Galvanised)	11.0	205	54
	11.0	410	27
	11.0	950	12
	5.0	1000	5
Split set SS46 (Nongalvanised)	15.0	280	54
	12.5	300	42
	16.0	500	32
	16.0	600	27
	29.0	1020	28
Inflatable bolt (Omega)	23.0	180	128
	32.5	1000	33
	23.0	200	115
	30.0	280	107
	32.0	1020	31

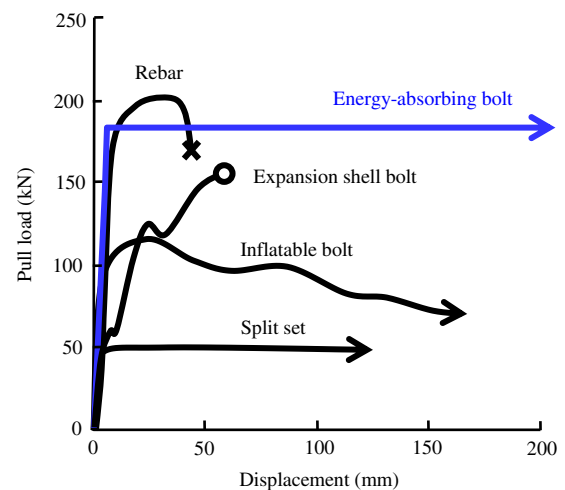


**Fig. 20.** Performance of different rockbolts subjected to pull loading. Redrawn after Stillborg (1994).

### 6.5. Interpretation of the pull test results with the loading models

The pull test results can be easily interpreted with the help of the rockbolt loading models presented in Section 2. For a mechanical bolt (Fig. 1), the axial load is identical at every cross-section of the bolt shank. Failure occurs at the weakest point of the bolt. The thread of the bolt is usually weaker than the shank. Thus failure usually occurs at the thread of the mechanical bolt or at the face plate if the latter is even weaker.

For a fully encapsulated rebar bolt, the maximum axial load occurs at the position where the pull load is applied (Fig. 2). The axial load decreases with distance from that position because of the shear stress at the bolt–grout interface. The shear stress on the bolt surface is related to the extent of de-bonding, completely de-bonding leading to a zero shear stress and partially de-bonding to a shear stress less than the ultimate one. The ultimate displacement of the rebar bolt is proportional to the de-bonding length which is usually quite short (approximately 15 cm). Therefore the rebar bolt fails after a very small displacement.

Similar to a rebar bolt, a frictional bolt has its maximum axial load at the position where the axial load is applied, but different from the former, and the latter has a constant shear stress in the “de-bonding” slippage section (Fig. 4). The frictional bolt slips and can accommodate large rock deformations when the bolt length is shorter than the critical embedment length of the bolt, but slippage will not occur and bolt shank will fail if the bolt length is longer than the critical embedment length. The critical embedment length of Split set is very long because of the low shear strength at the bolt–rock interface. Thus Split set always slips to accommodate rock dilation with its length used in practice (max. 3 m long, Fig. 11). As mentioned above, the critical embedment length of the inflatable bolts is approximately 1.5 m. An inflatable bolt would not slip and fail in rupture of the bolt tube if its embedment length is longer than 1.5 m.

## 7. Concluding remarks

The static and dynamic performances of conventional and energy-absorbing rockbolts are reviewed in this paper based on the results of laboratory tests carried out in the Rock Mechanics Laboratory at NTNU, as well as data reported in published literature. It is shown that mechanical bolts often fail at the plate, thread or inner anchor point, and are especially vulnerable to external disturbances such as vibrations. Anchoring reliability is also an issue for this type of rockbolt. Although a fully encapsulated rebar bolt can carry a high load, its displacement capacity is small. The advantage of this type of bolt is its reliable anchoring because of the full encapsulation. A frictional bolt can accommodate significant rock deformation, but can carry only a relatively small load. As the energy absorption of all conventional rockbolts is small, they are not appropriate for use as support devices in high rock stress conditions.

Energy-absorbing rockbolt is a new type of support device that has been attracted significant attention in recent years. An energy-absorbing bolt can both carry a high load and accommodate large rock displacement, and thus possesses a high energy-absorbing capacity. Such bolts are therefore desirable support devices in high rock stress conditions. The current energy-absorbing rockbolts absorb energy either through ploughing/slippage at predefined load levels or through stretching of the bolt steel. The dynamic load capacity of an energy-absorbing bolt with a ploughing/slippage-based displacement mechanism is usually smaller than its static load capacity.

## Conflict of interest

We wish to confirm that there are no known conflicts of interest associated with this publication and there has been no significant financial support for this work that could have influenced its outcome.

## References

- Cai M, Champaigne D. Development of a fully debonded cone bolt for rockburst support. In: Jan MVS, Potvin Y, editors. Deep Mining 2010 – Proceedings of the 5th International Seminar on Deep and High Stress Mining. Australian Centre for Geomechanics; 2010. pp. 329–42.
- Charette F, Plouffe M. Roofex – results of laboratory testing of a new concept of yieldable tendon. In: Potvin Y, editor. Deep Mining 07 – Proceeding of the 4th International Seminar on Deep and High Stress Mining. Australian Centre for Geomechanics; 2007. pp. 395–404.
- Cheng L, Feng S. Mechanism and strengthening effect of split set bolts. In: Proc. of Int. Symp. on Rock Bolting. Abisko; 1983. pp. 429–37.
- Dahle H, Larsen T. Full-scale pull and shear tests of 5 types of rockbolts. Trondheim: SINTEF; 2006.
- Galler R, Gschwandner GG, Doucet C. Roofex bolt and its application in tunnelling by dealing with high stress ground conditions. In: ITA-AITES World Tunnel Congress. Helsinki, Finland; 2011.
- Hadjigeorgiou J, Potvin Y. A critical assessment of dynamic rock reinforcement and support testing facilities. Rock Mechanics and Rock Engineering 2011;44(5): 565–78.
- Jager AJ. Two new support units for the control of rockburst damage. In: Kaiser PK, McCreath DR, editors. Proc. Int. Symp. on Rock Support in Mining and Underground Construction. Rotterdam: A.A. Balkema; 1992. pp. 621–31.
- Kaiser PK, McCreath DR, Tannant DD. Chapter 4: support functions and characteristics. In: Canadian rockburst support handbook. Sudbury, Canada: Geomechanics Research Centre; 1996. pp. 14–5.
- Li C, Stillborg B. Analytical models for rockbolts. International Journal of Rock Mechanics and Mining Sciences 1999;36(8):1013–29.
- Li CC. A new energy-absorbing bolt for rock support in high stress rock masses. International Journal of Rock Mechanics and Mining Sciences 2010;47(3): 396–404.
- Li CC. Design principles and desired performance of bolts for rock support in deep mining. In: The 6th Int. Symp. on Rockbolting in Mining and Injection Technology and Road Support Systems. Aachen: VGE Verlag GmbH; 2008. pp. 101–20.
- Li CC. Performance of D-bolts under static loading conditions. Rock Mechanics and Rock Engineering 2012;45(2):183–92.
- Li CC, Doucet C. Performance of D-bolts under dynamic loading conditions. Rock Mechanics and Rock Engineering 2012;45(2):193–204.
- Lindfors U. Test of the cone bolt in the Kristineberg mine. Sweden: Boliden Mineral AB; 2000. B2/00.
- Myrvang A, Hanssen TH. Experiences with friction rock bolts in Norway. In: Proc. of Int. Symp. on Rock Bolting. Abisko; 1983. pp. 419–23.
- Ortlepp WD. The design of support for the containment of rockburst damage in tunnels – an engineering approach. In: Kaiser PK, McCreath DR, editors. Proc. Int. Symp. on Rock Support in Mining and Underground Construction. Rotterdam: A.A. Balkema; 1992. pp. 593–609.
- Player JR, Thompson AG, Villaescusa E. Dynamic testing of reinforcement system. In: Proceedings 6th International Symposium on Ground Support in Mining and Civil Engineering Construction, SAIMM Symposium Series S51; 2008. pp. 581–95.
- Player JR, Villaescusa E, Thompson AG. Dynamic testing of friction rock stabilisers. In: Diederichs M, Grasselli G, editors. Proc. of the 3rd Canada–US Rock Mechanics Symposium; 2009.
- Simser B. Geotechnical review of the July 29th, 2001 West Ore Zone Mass Blast and the performance of the Brunswick/NTC rockburst support system. Technical report; 2001.
- Simser B, Andrieux P, Langevin F, Parrott T, Turcotte P. Field behaviour and failure modes of modified conebolts at the Craig, LaRonde and Brunswick Mines in Canada. In: Deep and High Stress Mining; 2006. Quebec City, Canada.
- Stillborg B. Professional users handbook for rock bolting. 2nd ed. Clausthal-Zellerfeld, Germany: Trans. Tech. Publications; 1994.
- Stjern G. Practical performance of rockbolts. PhD Thesis. Trondheim: Norwegian University of Science and Technology; 1995. p. 52.
- Varden R, Lachenicht R, Player J, Thompson A, Villaescusa E. Development and implementation of the Garford dynamic bolt at the Kanowna Belle Mine. In: 10th Underground Operators Conference. Launceston; 2008. pp. 95–102.
- Windsor CR. Rock reinforcement systems. International Journal of Rock Mechanics and Mining Sciences 1997;34(6):919–51.
- Wu YK, Oldsen J, Lamothe M. The Yield-Lok bolt for bursting and squeezing ground support. In: Jan MVS, Potvin Y, editors. Deep Mining 2010 – Proceedings of the 5th International Seminar on Deep and High Stress Mining. Australian Centre for Geomechanics; 2010. pp. 301–8.



**Dr. Charlie Chunlin Li** is professor of rock mechanics for civil and mining engineering at the Norwegian University of Science and Technology (NTNU) in Norway. Li received his BSc degree in 1981 and MSc degree in 1984, both in geological engineering, in Central South Institute of Mining and Metallurgy (at present Central South University), and his PhD in mining rock mechanics at Luea University of Technology (LUT), Sweden, in 1993. After that, he was employed as research associate and then associate professor at LUT until 2000. He worked then in the Kristineberg mine of Boliden Mineral Ltd., Sweden, as mining engineer for 4 years. He has chaired the professor in rock mechanics at NTNU since 2004, in charge of the teaching and research program in the subject of rock mechanics as

well as the rock mechanics laboratory. He is a member of the Norwegian Academy of Technological Sciences (NTVA). Prof. Li's research interests are in rock failure, stability analysis of underground spaces, ground support and application of rock mechanic principles for underground space design. He developed a constitutive model for brittle rock materials to take into account the effects of microcracks and cracking on the nonlinear behaviour of the rock. He carried out a thorough laboratory study of the acoustic Kaiser effect in rock materials and concluded that the Kaiser effect is a measure of damage in the rock. He is now focussing on experimental and numerical studies of brittle rock failure under low confining pressure, including spalling, slabbing and rockburst. After a thorough study of the performances of rockbolts, he proposed

three analytical models for rockbolts in accordance with their anchoring mechanisms. The models are now frequently cited and used by others and are widely acknowledged in the circle of rock mechanics. With the help of his analytical models, Li identified the shortcomings of the conventional rockbolts and found ways to overcome them. His research of rockbolt finally led to the invention of a new type of yield rockbolt, called D-Bolt. The D-Bolt is characterised by its high load capacity and high deformability. In other words, the bolt is able to absorb a good amount of deformation energy prior to failure. The bolt is particularly powerful in combating stress-induced rockburst and rock squeezing. The technology has been welcomed by the mining and tunnelling industry since it was born. NTNU established a company – Dynamic Rock Support (DRS) in 2009 to commercialise the new technology. DRS was acquired by a giant underground equipment company – Normet after 4 years because of the bright market of the bolt in the world. The D-Bolt is being used today world-widely, for instance in Sweden, Canada, USA, Chile, Australia and South Africa, to combat instability problems in deep mines. Prof. Li received an innovation prize – Northern Lights Award by Raw Material Group for the D-Bolt technology in 2013 in Sweden. Prof. Li has practical expertise in ground support in difficult rock conditions (for instance rock squeezing and rockburst), stability analysis of underground caverns and in-situ measurements and interpretation. In the past years, he was involved in consulting work in a number of underground mining and excavation projects, for instance, rock support in burst-prone rock in LKAB's mines, rock support in squeezing and burst-prone rock in Boliden's mines and stability analysis and rock support for two hydropower underground caverns in squeezing rock in Himalayas.